Cardiac Lymphatic Dysfunction Causes Drug-Eluting Stent–Induced Coronary Hyperconstricting Responses in Pigs In Vivo

Hirokazu Amamizu, Yasuharu Matsumoto, Susumu Morosawa, Kazuma Ohyama, Hironori Uzuka, Michinori Hirano, Kensuke Nishimiya, Yusuke Gokon, Tomomi Watanabe-Asaka, Moyuru Hayashi, Satoshi Miyata, Takashi Kamei, Yoshiko Kawai, Hiroaki Shimokawa

Objective—We have previously demonstrated that coronary adventitial inflammation plays important roles in the pathogenesis of coronary vasomotion abnormalities, including drug-eluting stent (DES)–induced coronary hyperconstricting responses. Importantly, the adventitia also harbors lymphatic vessels, which may prevent inflammation by transporting extravasated fluid and inflammatory cells. We thus aimed to examine the roles of coronary adventitial lymphatic vessels in the pathogenesis of DES-induced coronary hyperconstricting responses in a porcine model in vivo.

Approach and Results—We performed 2 experimental studies. In protocol 1, 15 pigs were divided into 3 groups with or without DES and with bare metal stent. Nonstented sites 20 mm apart from stent implantation also were examined. In the protocol 2, 12 pigs were divided into 2 groups with or without lymphatic vessels ligation followed by DES implantation at 2 weeks later (n=6 each). We performed coronary angiography 4 weeks after DES implantation, followed by immunohistological analysis. In protocol 1, the number and the caliber of lymphatic vessels were greater at only the DES edges after 4 more weeks. In protocol 2, coronary hyperconstricting responses were further enhanced in the lymphatic vessels ligation group associated with adventitial inflammation, Rho-kinase activation, and less adventitial lymphatic vessels formation. Importantly, there were significant correlations among these inflammation-related changes and enhanced coronary vasoconstricting responses.

Conclusions—These results provide evidence that cardiac lymphatic vessel dysfunction plays important roles in the pathogenesis of coronary vasoconstrictive responses in pigs in vivo.

Visual Overview—An online visual overview is available for this article. **(*Arterioscler Thromb Vasc Biol*. 2019;39:741-753. DOI: 10.1161/ATVBAHA.119.312396.)**

Key Words: coronary vasospasm ■ drug-eluting stent ■ inflammation ■ lymph ■ Rho kinase

Despite recent advances in the medical management for ischemic heart disease, intractable vasospastic angina and unremitting angina because of coronary hyperconstricting responses even after successful percutaneous coronary intervention with drug-eluting stent (DES) are emerging clinical issues.[1–6] We have previously demonstrated that activation of Rho-kinase, a molecular switch for vascular smooth muscle contraction, plays a key role in the pathogenesis of coronary vasospasm and hyperconstricting responses after DES implantation in animals and humans.[2,3,7,8] We also have demonstrated that adventitial inflammatory changes play important roles in the pathogenesis of coronary spasm in pigs and humans.[9–14] Importantly, the adventitia harbors a variety of components, including not only vasa vasorum (VV) but also lymphatic vessels.[15]

The lymphatic vasculature collects interstitial fluid, macromolecules, and extravasated leukocytes from tissues.[16] Lymphatic vessels are essential for the development of inflammation, and edema occurs in inflammation when the rate of plasma leakage from blood vessels exceeds the drainage through lymphatic vessels.[17] Indeed, airway inflammation leads to bronchial lymphedema and exaggerates airflow obstruction in mice.[17] In addition, VEGF (vascular endothelial growth factor)-C (lymphangiogenic factor) reduces chronic skin inflammation in mice.[18] Notably, recent studies suggested that lymphatic vessels play important roles in the cardiovascular

Received on: November 4, 2018; final version accepted on: February 15, 2019.

From the Department of Cardiovascular Medicine (H.A., Y.M., S. Morosawa, K.O., H.U., M. Hirano, K.N., S. Miyata, H.S.) and Department of Gastroenterological Surgery (Y.G., T.K.), Tohoku University Graduate School of Medicine, Sendai, Japan; and Division of Physiology, Tohoku Medical and Pharmaceutical University (T.W.-A., M. Hayashi, Y.K.), Sendai, Japan.

This article was sent to Karin Bornfeldt, Consulting Editor, for review by expert referees, editorial decision, and final disposition.

The online-only Data Supplement is available with this article at https://www.ahajournals.org/doi/suppl/10.1161/ATVBAHA.119.312396.

Correspondence to Hiroaki Shimokawa, MD, PhD, Department of Cardiovascular Medicine, Tohoku University Graduate School of Medicine, 1-1, Seiryo-machi, Aoba-ku, Sendai 980-8574, Japan. Email shimo@cardio.med.tohoku.ac.jp

Nonstandard Abbreviations and Acronyms

BMS	bare metal stent
CAG	coronary angiography
CD68	cluster of differentiation 68
DES	drug-eluting stent(s)
IC	intracoronary injection
ICG	indocyanine green
IL-1β	interleukin-1β
LYVE-1	lymphatic vessel endothelial hyaluronan receptor 1
p-MYPT1	phosphorylated myosin phosphatase target subunit 1
ROCK	Rho-associated coiled-coil containing protein kinase
VV	vasa vasorum

disease.[15,19,20] The number of adventitial lymphatic vessels increases associated with intimal thickness of human carotid arteries.[21] Lymphatic vessels are also involved in the development of atherosclerosis.[22] However, since the discovery of the cardiac lymphatic system by Rudbeck in 1653,[23,24] little attention has been paid to the roles of cardiac lymphatic vessels in the pathogenesis of coronary vasomotion abnormalities.

In the present study, we thus performed experimental studies to examine the roles of cardiac lymphatic vessels in the pathogenesis of coronary spasm using an established porcine model with hyperconstricting responses after DES implantation in vivo.[1,3,7,8,25–27]

Materials and Methods

All data and supporting materials have been provided with the published article.

Study Protocol

We performed 2 experimental protocols. All animal care and experimental studies were performed in accordance with the Guide for the Care and Use of Laboratory Animals published by the US National Institute of Health (NIH Publication, 8th Edition, 2011) and were approved by the Institutional Committee for Use of Laboratory Animal of Tohoku University (No 2017MdA-139).

In the protocol 1, we examined the changes in adventitial lymphatic vessels in a porcine model of DES-induced coronary hyperconstricting responses in vivo (Figure 1A). In the protocol 2, we examined the effects of cardiac lymphatic vessels ligation on coronary vasomotion (Figure 1B).

Protocol 1

In our animal facility, the light is turned on at 8 o'clock and turned off at 18 o'clock. Pigs can freely drink water at any time and eat normal diet (Grandeal B; Zennoh Feed Mills of the Tohoku Distinct, Miyagi, Japan) 3× every day. Ten male pigs (BW, 35–45 kg) were orally pretreated with aspirin (200 mg/day, PO) and clopidogrel (225 mg/day, PO) for 2 days before stent implantation (Figure 1A).[25] After sedation with medetomidine (0.1 mg/kg, IM) and midazolam (0.2 mg/kg, IM), followed by inhaled sevoflurane (2%–5%) and heparinization (5000 U, IV), each animal underwent a DES (everolimus-eluting stent) implantation. DES was implanted into the left anterior descending coronary artery in 5 pigs, and the remaining 5 pigs did not undergo stent implantation as a control group. At 1 month after DES implantation, we performed coronary angiography (CAG) to examine coronary vasomotion in vivo. After the CAG study, the animals were euthanized with a lethal dose of potassium chloride (0.25 mEq/kg, IV) under deep anesthesia with inhaled 5% sevoflurane.

To evaluate the specific effect of the DES, we also histologically examined the coronary artery of pigs implanted with bare metal stent (BMS), as previously reported.[27] They were pretreated orally with aspirin and clopidogrel for 2 days before stent implantation. After sedation with medetomidine and midazolam, followed by inhaled sevoflurane and heparinization, we implanted BMS into the left coronary artery (n=5). At 1 month after BMS implantation, they were euthanized with a lethal dose of potassium chloride and the heart was removed.

Protocol 2

Twelve male pigs (BW 35–40 kg) (Major Resources Table in the online-only Data Supplement) were randomly divided into 2 groups: cardiac lymphatic vessels ligation group and the sham group (N=6 each; Figure 1B). After sedation with medetomidine (0.1 mg/kg, intramuscular injection) and midazolam (0.2 mg/kg, intramuscular injection), followed by inhaled sevoflurane (2%–5%) and heparinization (5000 U, IV), a left thoracotomy was performed in the third intercostal space, and 0.1 mL of Evans blue was injected into the myocardium to visualize the lymphatic vessels.[28,29] The cardiac lymphatic vessels close to the proximal right and left main coronary arteries were ligated with 7-0 nylon threads and were transected between the ligatures on each lymphatic vessel in the ligation group. Sham animals underwent the same open-chest surgical procedures as the ligation group but without lymphatic vessels ligation or resection of lymphatic vessels. After closing the chest in both groups with 2-0 vicryl thread, we inserted a central venous catheter into the internal jugular vein for high calorie infusion and antibiotics for 3 to 4 days thereafter. For 12 days after the operation, the animals were treated with aspirin (200 mg/day, PO) and clopidogrel (225 mg/day, PO). Two days after the start of the dual antiplatelet therapy, they underwent DES implantation into the left anterior descending coronary arteries. No significant differences were noted in the procedure parameters for DES implantation between the sham and the ligation groups (Table I in the online-only Data Supplement). At 1 month after DES implantation, we performed CAG study to examine coronary vasomotion in pigs in vivo. After the CAG study, we performed median thoracotomy and lymphatic vessels ligation and examined cardiac lymph transport with injection of indocyanine green (ICG, 0.2 mL, Diagnogreen 25 mg; Daiichi Pharmaceutical, Tokyo, Japan) with the photodynamic eye (PDE) near-infrared camera system (Hamamatsu Photonics, Hamamatsu, Japan).[30] The speed was calculated by the following formula: [the length of ICG diffusion divided by time constant].[31] After these studies, the animals were euthanized with a lethal dose of potassium chloride (0.25 mEq/kg, IV) under deep anesthesia with inhaled 5% sevoflurane.

Coronary Angiographic Study

After control CAG, we examined coronary vasoconstricting responses to serotonin (10 and 100 μg/kg, IC) before and after intracoronary hydroxyfasudil (30 and 300 μg/kg, slow IC for 3 min), a specific Rho-kinase inhibitor (Asahi Kasei Pharma, Tokyo, Japan).[1,3,7,25–27] Coronary vasodilating responses to nitroglycerin (10 μg/kg, IC) and bradykinin (0.1 μg/kg, IC) before and after N^G-monomethyl-L-arginine (1 mg/kg, slow IC for 10 min) were examined. Quantitative comparative analysis was performed in a blind manner at the proximal and distal stent edge segments adjacent to the stent as previously described.[3,7,8,25,26]

Histological Analysis

The paraffin sections of coronary arteries in the stent edge sites (5 mm apart from the stent) in the protocols 1 and 2,[8,25] and the nonstented sites (20 mm apart from the stent edges; DES+20) in the protocol 1 were cut into a 3-μm-thick slice. They were stained with Masson's trichrome staining and hematoxylin eosin staining. Histomorphometric parameters were manually measured by using Image-J (US National Institute of Health, Bethesda, MD). Adipocyte size was evaluated as mean diameter (μm) in the perpendicular maximum and minimum axes, and the data were represented as an average of each adipocyte in 3 random high-power fields.[25,32,33] In the protocol 2, myocardium slices were stained with Masson's trichrome staining to assess the influence of lymphatic vessels ligation on myocardial fibrosis. Collagen volume fraction, expressed as percentage of fibrosis area per microscopic field by using Image J, was used to express the extent of myocardial fibrosis.[34] Overall thickness of the atrioventricular valve leaflets was averaged

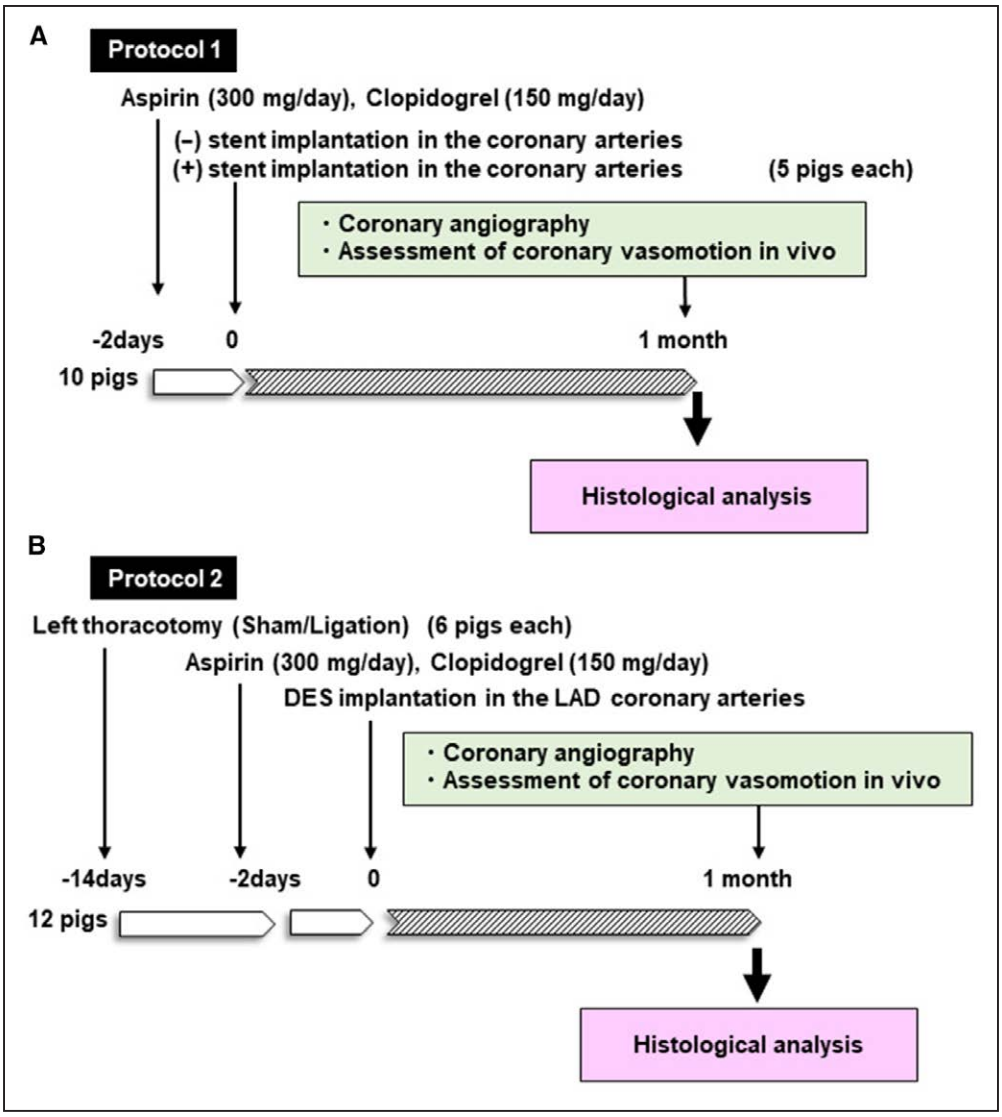

Figure 1. In the protocol 1 (**A**), 10 pigs were pretreated orally with aspirin (200 mg/day, PO) and clopidogrel (225 mg/day, PO). Two days after the start of the dual antiplatelet therapy, a stent was implanted into the left coronary artery in 5 pigs, and the remaining 5 pigs did not undergo stent implantation as a control group. At 1 mo, all animals underwent coronary angiography followed by histological analysis. In the protocol 2 (**B**), 12 domestic pigs underwent left thoracotomy and were randomly divided into 2 groups, cardiac lymphatic vessels ligation group and the sham group (N=6 each). For 12 days after the operation, the animals were treated with aspirin (200 mg/day, PO) and clopidogrel (225 mg/day, PO). Two days after the start of the dual antiplatelet therapy, all animals underwent drug-eluting stent (DES) implantation into the left anterior descending (LAD) coronary arteries. At 1 mo after DES implantation, all animals underwent coronary angiography followed by histological analysis.

over 5 equally distributed length measurements throughout the valve and was quantified by using Image J, as previously described.[35]

Immunohistological Analysis

Immunohistological staining was performed on paraffin-embedded tissue sections using rabbit anti-LYVE-1 (lymphatic vessel endothelial hyaluronan receptor-1; 1:10000, RF2219633; Thermo Fisher Scientific, Waltham, MA) antibody for lymphatic vessels (Major Resources Table in the online-only Data Supplement). Immunohistological staining was performed with rabbit anti-human VWF (von Willebrand factor) antibody (N1505; DAKO, Copenhagen, Denmark) for VV and rabbit anti-tyrosine hydroxylase (BIO RAD; Hercules, CA) for sympathetic nerve fibers. The densities of lymphatic vessels, VV, and sympathetic nerve fibers were expressed as a number of LYVE-1-positive, VWF-positive vessels, and tyrosine hydroxylase–positive fibers divided by the adventitial area (/mm^2), respectively.[26,36–38] The quantification of lymphatic vessel caliber were performed manually using Image-J software.[39] Adventitial area was calculated by the following formula: [area outside the external elastic lamina within a distance of the thickness of neointima plus media–external elastic lamina area]. Immunohistological staining was also performed with anti-rabbit adiponectin antibody (1:50; No. AA605Po01; Cloud-clone Corp, Wuhan, China) (Major Resources Table in the online-only Data Supplement).[25] Quantitative analysis of adiponectin was evaluated as positive staining area in perivascular adipose tissue, which was calculated by the following formula: positive staining area/total area at 100× magnification using the AxioVision Software (Release 4.5, Zeiss, Jena, Germany). The percentage of positive staining area for adiponectin in perivascular adipose tissue was calculated as an average of 3 random high-power fields.[25] Immunohistological staining was also performed with mouse anti-cluster designation (CD68 [cluster of differentiation 68]) antibody (ED1, 1:50; ab31630; Abcam, Cambridge, UK) (Major Resources Table in the online-only Data Supplement) for macrophages, and goat anti-human IL (interleukin)-1β (1:50; AB-201-NA; R&D Systems,

Minneapolis, MA) (Major Resources Table in the online-only Data Supplement). The numbers of CD68- and IL-1β-positive cells in the coronary adventitia were calculated as an average of 3 random high-power fields. Immunohistochemical staining was also performed with mouse anti-human Rho-kinase β (ROCK1 [Rho-associated coiled-coil containing protein kinase]; 1:50; 61136; BD Biosciences, San Jose, CA) (Major Resources Table in the online-only Data Supplement), mouse anti-Rho-kinase α (ROCK2) antibodies (1:50; 610624; BD Biosciences) (Major Resources Table in the online-only Data Supplement), rabbit anti-human phosphorylated myosin phosphatase target subunit-1 (pMYPT1) antibody (1:50; 07-251; Millipore, Billerica, MA) (Major Resources Table in the online-only Data Supplement), a substrate of Rho-kinase. Each section was divided into a total of 12 radial subparts. Semiquantitative analysis of the extent of ROCK1, ROCK2, and pMYPT1 was evaluated for each radial subpart per one section by using the following scale: 0, none; 1, slight; 2, moderate; and 3, high, as previously described.[8,25–27] As negative control antibodies, we used rabbit immunogloblin fraction (No. X0903; DAKO) for LYVE-1, adiponectin, and pMYPT1; mouse IgG1 (No. X0931, DAKO) for CD68, ROCK1, and ROCK2; and mouse IgG isotype control (No. bs-0294; Bioss, Woburn, MA) for IL-1β.

Statistical Analysis

Results are expressed as mean±SEM. Throughout the text and figures, N represents the number of pigs, while n represents the number of DES edges in the protocols 1 and 2. In the protocol 2, we performed hierarchical clustering with Pearson's correlation as similarity coefficient and the Ward clustering method to examine the individual difference in the proximal and distal stent edges in a pig. In this analysis, the values of coronary vasoconstricting responses and histological analysis at the edges were used for clustering, and no evident cluster of proximal/distal pairs of same pig was noted (Figure I in the online-only Data Supplement). Based on this analysis, various changes at the proximal and distal edges in a pig were treated as individual factors in the protocol 2. A comparison of the quantitative comparative analysis and histomorphometry was performed by using Welch *t* test for unequal variances. Comparison of the semiquantitative analysis was performed by using a Mann-Whitney *U* test. In some comparisons, the distributions of the groups were not normal and they were heteroscedastic. To improve the normality and stabilize the variances of the distributions, the BOX-Cox transformation was applied. Then the equality of the variances and the normality of the distributions were confirmed by the Bartlett test of homogeneity of variances and the Shapiro-Wilk normality test, respectively. Comparison of the semiquantitative analysis was performed by using a Mann-Whitney *U* test. In addition, a comparison of histomorphometry of control, DES and BMS, or control, DES and DES+20 in the protocol 1 was performed by one-way ANOVA for the transformed data by the Box-Cox method followed by the multiple comparison using Tukey Honestly Significant difference. The correlation between the continuous variables was analyzed using a linear regression model. Statistical analysis was performed with IBM SPSS Statistics 20 (IBM, New York, NY) and R version 3.5.1. A value of $P<0.05$ was considered to be statistically significant.

Results

Protocol 1. Effects of DES Implantation on Adventitial Lymphatic Vessels and Inflammation

In the protocol 1, at 1 month after DES implantation, coronary hyperconstricting responses were noted at the DES edges compared with the control site, as previously reported.[25] Histological analysis showed that adventitial LYVE-1-positive lymphatic vessels appeared more evident at the DES edges compared with the control sites and BMS edges (Figure 2A through 2F). Indeed, quantitative analysis showed that the number and the caliber of LYVE-1-positive lymphatic vessels were significantly more and larger at the DES edges compared with the control group and BMS edges (Figure 2I and 2J). Histological analysis showed that adventitial lymphatic vessels appeared more evident at the DES edges compared with control and DES+20 sites (Figure 2A through 2D, 2G, and 2H). Indeed, quantitative analysis showed that the number and the caliber of lymphatic vessels were significantly more and larger at the DES edges compared with the control and DES+20 sites (Figure 2K and 2L). There were significant correlations between the number of lymphatic vessels and IL-1β-positive cells (Figure 2M) and vasoconstriction to serotonin in control sites and DES edges (Figure 2N).

Protocol 2. Effects of Cardiac Lymphatic Vessels Ligation on Coronary Hyperconstricting Responses

In the protocol 2, we performed cardiac lymphatic vessels ligation, in which the ligation points of cardiac lymphatic vessels were clearly visualized with Evans blue (Figure 3A). At 1 month after DES implantation, we performed ICG injection study followed by CAG study. In the ICG study, lymph transport of ICG was clearly noted from the apex to the base in the sham group, whereas ICG remained at the apex in the ligation group (Figure 3B). Indeed, lymph transport speed was markedly reduced in the ligation group than in the sham group (Figure 3C). In the CAG study, no in-stent restenosis was noted in both groups (Figure 4A and 4D). Notably, coronary vasoconstricting responses to intracoronary serotonin were enhanced at the proximal and distal DES edges in the ligation group compared with the sham group, which were abolished by intracoronary pretreatment with hydroxyfasudil (Figure 4B, 4C, 4E, and 4F). Quantitative CAG analysis demonstrated that coronary vasoconstricting responses to serotonin were significantly enhanced in the ligation group compared with the sham group (Figure 4G). In contrast, endothelium-independent and -dependent coronary vasodilating responses to nitroglycerin and bradykinin (regardless of the presence or absence of N^G-monomethyl-L-arginine) were comparable between the 2 groups (Table II in the online-only Data Supplement).

Effects of Cardiac Lymphatic Vessel Ligation on Coronary Adventitial Inflammation and Rho-Kinase Activity

Immunohistological and subsequent quantitative analyses showed that LYVE-1-positive lymphatic vessels at the DES edges appeared less and smaller in the ligation group compared with the sham group (Figure 5A, 5B, 5E, 5F, 5I, and 5J). Masson's trichrome staining showed that adipocyte size was significantly larger in the ligation group compared with the sham group (Figure 5C, 5G, and 5K). In contrast, adiponectin-positive areas (%) were significantly reduced in the ligation group compared with the sham group (Figure 5D, 5H, and 5L). There was a significant negative correlation between the number of lymphatic vessels and adipocyte size (Figure 5M).

Inflammatory cells (macrophages and IL-1β-positive cells) in the adventitia at the DES edges were noted in the ligation group more than in the sham group (Figure 6A through 6H). In contrast, there was no significant difference in the number of VV or sympathetic nerve fibers between the 2 groups (VV, sham 34.9±2.7/mm^2 versus ligation 30.8±4.2/mm^2, P=0.43;

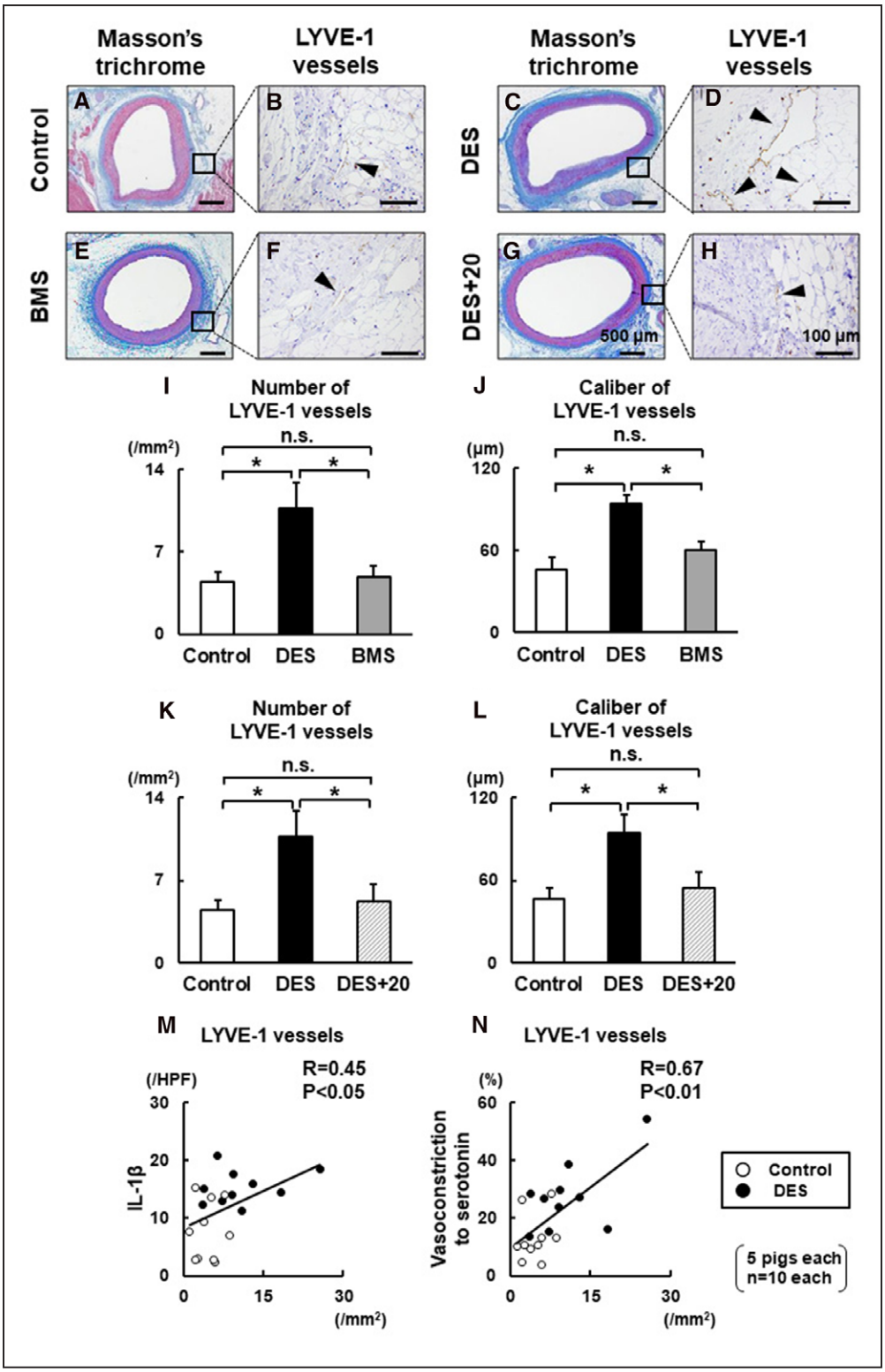

Figure 2. Lymphatic vessels at the coronary adventitia in a pig without drug-eluting stent (DES) implantation as a control (**A** and **B**), those at the DES edge of the coronary artery (**C** and **D**), those at the bare metal stent (BMS) edge of the coronary artery (**E** and **F**), and those at the DES+20 sites (**G** and **H**), as indicated by black arrow heads. Quantitative analysis of lymphatic vessels in the coronary adventitia among the control, DES, and BMS groups (**I** and **J**), and among the control, DES, and DES+20 groups (**K** and **L**). Correlations between the number of lymphatic vessels and IL (interleukin)-1β–positive cells (**F**) and between the number of lymphatic vessels and vasoconstriction to serotonin (**G**). Results are expressed as mean±SEM. **P*<0.05. HPF indicates high-power field; and LYVE, lymphatic vessel endothelial hyaluronan receptor-1.

sympathetic nerve fibers, sham 9.9±1.3/mm^2 versus ligation 8.2±2.3/mm^2, *P*=0.52). Immunoreactivities for ROCK1/2 and pMYPT1 were predominantly noted in the medial vascular smooth muscle cells (Figure 6I through 6P), and semiquantitative analysis showed that the expressions of ROCK1/2 and pMYPT1 at the DES edges were significantly enhanced in the

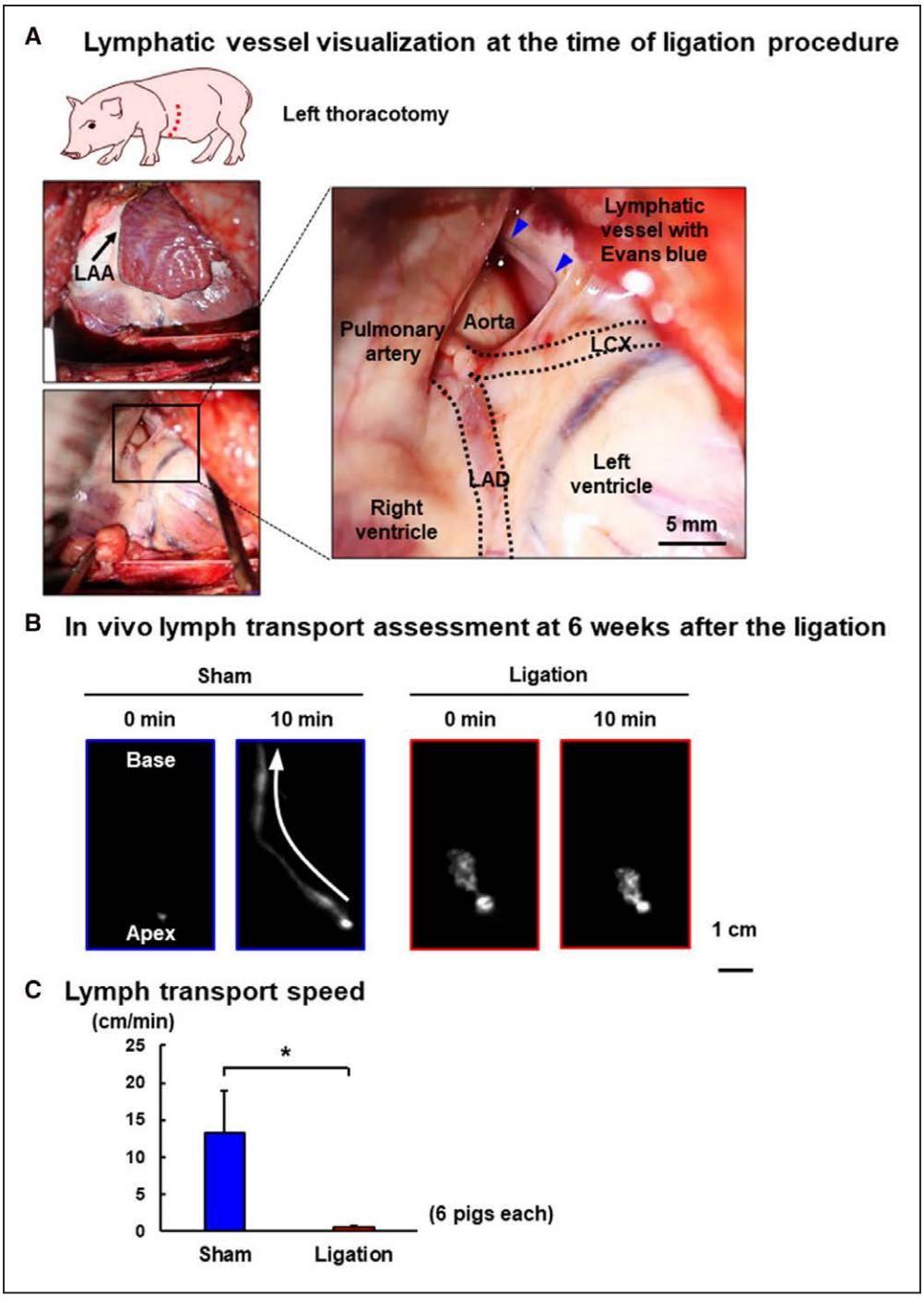

Figure 3. Representative pictures of cardiac lymphatic vessel visualization with Evans blue dye at the time of sham or ligation procedure after left thoracotomy (**A**). After turning over left atrial appendage (LAA; **A**, **left**), cardiac lymphatic vessels were visualized with Evans blue (**A**, **right**). Blue arrow heads indicate the ligation points of cardiac lymphatic vessel. In vivo lymph transport assessment with indocyanine green (ICG) injection at 6 wk after the sham or ligation procedure (**B**) and lymph transport speed (**C**). White arrow indicates the lymph transport of ICG from apex to the base in the sham group. **P*<0.05 sham vs ligation. LAD indicates left anterior descending coronary artery; and LCX, left circumflex coronary artery.

ligation group than in the sham group (Figure 6Q through 6S). There was a significant positive correlation between adipocyte size and the number of IL-1β-positive cells (Figure 6T). Furthermore, significant positive correlations were noted between the number of IL-1β-positive cells and pMYPT1 expression (Figure 6U) and between pMYPT1 levels and the extent of coronary vasoconstriction to serotonin (Figure 6V).

Effects of Cardiac Lymphatic Vessels Ligation on Myocardium and Atrioventricular Valves

Masson's trichrome staining showed that the extent of myocardial fibrosis was significantly increased in the ligation group compared with the sham group (Figure IIA, IIB, and IIG in the online-only Data Supplement). In addition, the thicknesses of tricuspid and mitral valves were also significantly greater in

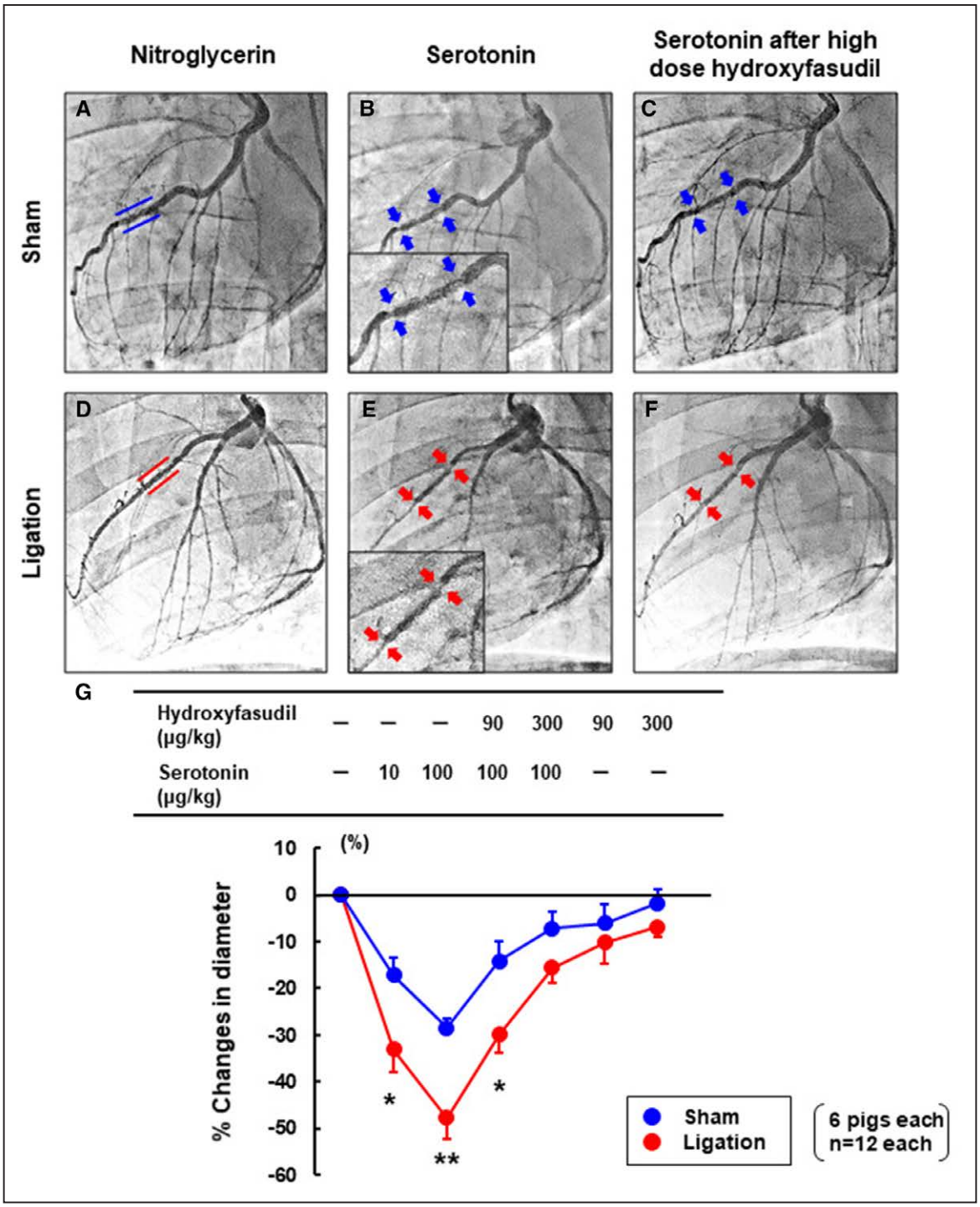

Figure 4. Representative left coronary angiograms in pigs after nitroglycerin (**A** and **D**), serotonin (**B** and **E**), and serotonin after pretreatment with hydroxyfasudil (**C** and **F**) at 6 wk after the sham or ligation procedure, and the results of quantitative coronary angiography regarding coronary vasoconstricting responses to serotonin (10 and 100 μg/kg, IC) before and after hydroxyfasudil (90 and 300 μg/kg, IC; **G**). The blue and red lines represent drug-eluting stent (DES) implantation sites in the left anterior descending (LAD) coronary arteries. The mean value of coronary vasoconstricting responses of the proximal and the distal DES edges are presented. Results are expressed as mean±SEM. **P*<0.05, ***P*<0.01 sham vs ligation.

the ligation group than in the sham group (Figure IIC through IIF, IIH, and II-I in the online-only Data Supplement).

Negative Controls for Immunohistochemistry

Negative controls of immunohistochemistry were performed for LYVE-1, adiponectin, CD68, IL-1β, ROCK1, ROCK2, and pMYPT1 (Figure IIIA through IIIN in the online-only Data Supplement).

Discussion

The major findings of the present study were as follows: (1) In the present study with pigs, enhanced lymphatic vessel

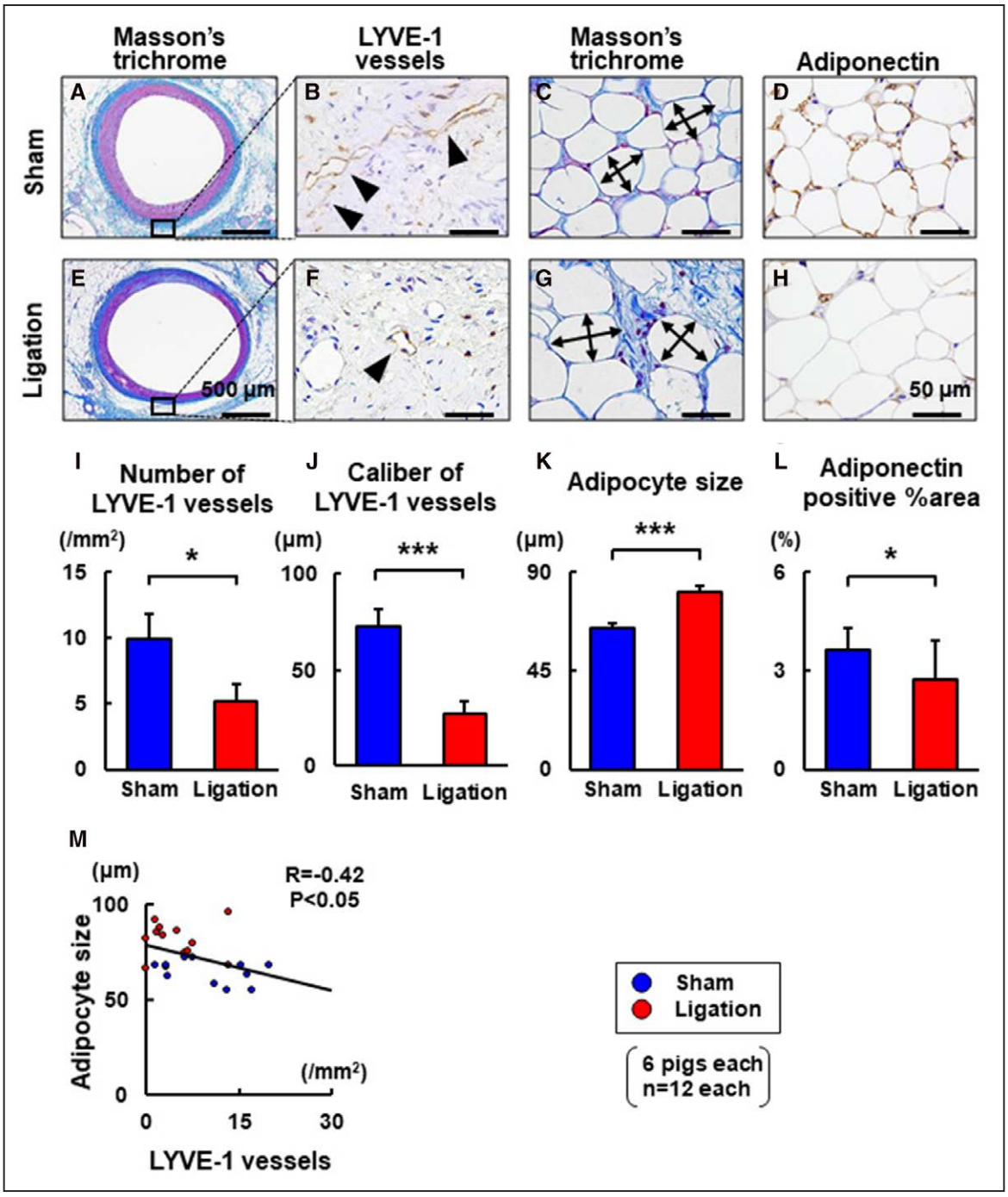

Figure 5. Representative pictures at the drug-eluting stent (DES) edges for Masson's trichrome staining (**A** and **E**) and immunostainings of LYVE-1 (lymphatic vessel endothelial hyaluronan receptor-1; **B** and **F**), adipocytes with Masson's trichrome staining (**C** and **G**), and adiponectin (**D** and **H**). Black arrow heads indicate lymphatic vessels, and arrows indicate the diameters in the perpendicular maximum and minimum axes. Quantitative histological analysis between the 2 groups (**I**–**L**) and correlation between the number of LYVE-1 vessels and adipocyte size is shown **M**. Results are expressed as mean±SEM. **P*<0.05, ****P*<0.001 sham vs ligation.

formation was noted at the DES edges associated with coronary vasoconstricting responses but not at the BMS edges or DES+20 mm sites. (2) Lymphatic vessels ligation further enhanced coronary hyperconstricting responses after DES implantation. (3) Lymphatic vessels ligation decreased the number of lymphatic vessels, although there were no significant differences in the number of VV between the sham and the ligation groups. (4) Lymphatic vessels ligation caused adipocyte hypertrophy associated with enhanced inflammation in the adventitia and Rho-kinase activation. This study demonstrates the important roles of cardiac lymphatic vessels in the pathogenesis of coronary hyperconstricting responses and cardiac structural changes.

Effects of Stent Implantation on the Density and Caliber of Lymphatic Vessels

We examined the density and the caliber of lymphatic vessels at the control sites and at the DES and BMS edges. Histological

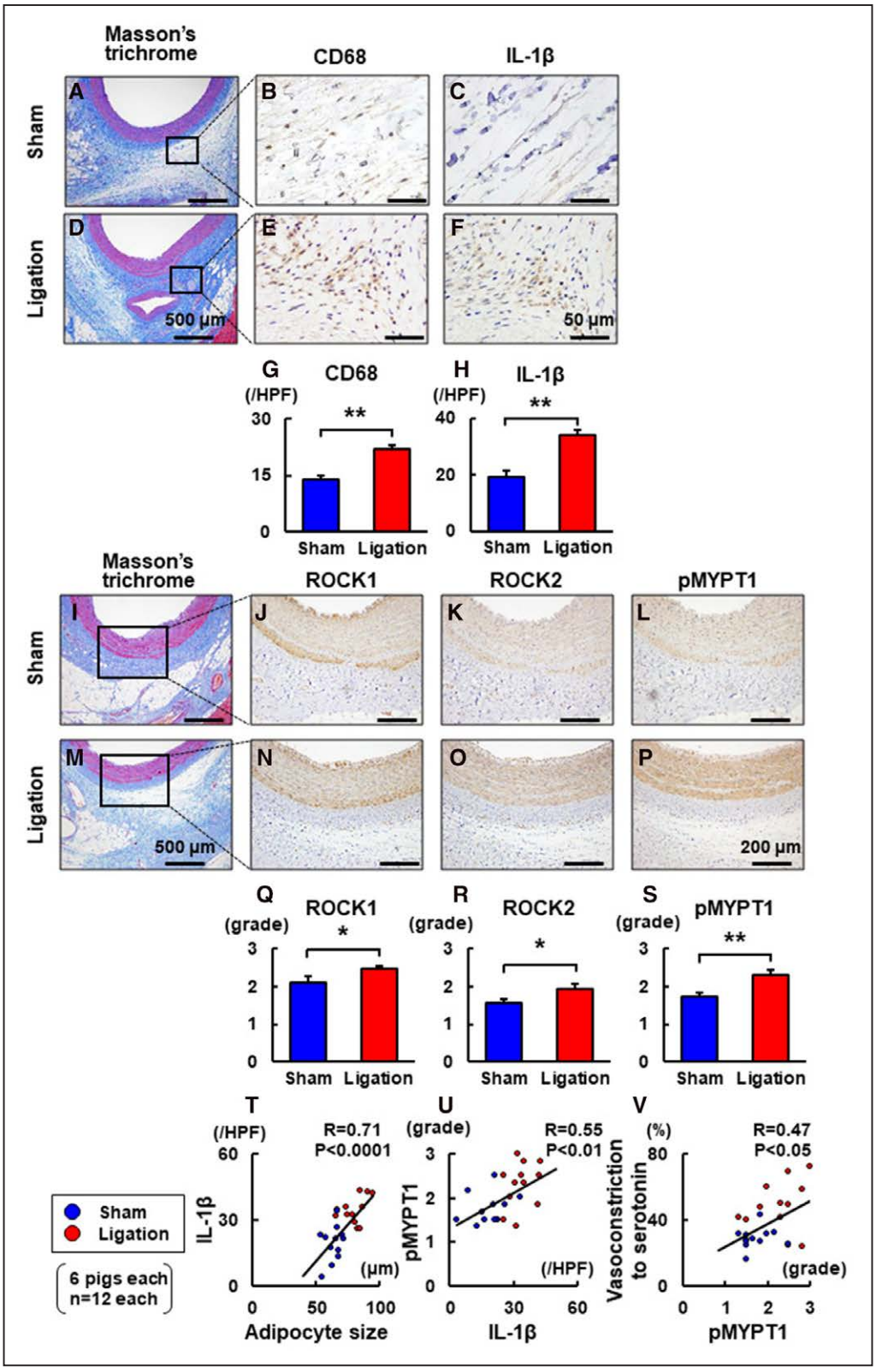

Figure 6. Representative pictures at the drug-eluting stent (DES) edges for Masson's trichrome staining (**A**, **D**, **I**, and **M**) and immunostainings of CD68 (cluster of differentiation 68; **B** and **E**), IL (interleukin)-1β (**C** and **F**), ROCK1 (**J** and **N**), ROCK2 (**K** and **O**), and pMYPT1 (**L** and **P**). Quantitative histological analysis and correlations among the histological results and the extent of coronary vasoconstriction are shown (**G**, **H**, and **Q**–**V**). Results are expressed as mean ± SEM. *P<0.05, **P<0.01, Sham vs. Ligation. HPF indicates high-power field; p-MYPT1, phosphorylated myosin phosphatase target subunit 1; and ROCK, Rho-associated coiled-coil containing protein kinase.

analysis showed that the number and the caliber of lymphatic vessels were significantly greater at the DES edges compared with the control and the BMS edges, whereas there was no significant difference between the control and the BMS sites. These results indicate that DES, but not BMS, affect lymphatic vessels in the coronary adventitia. Histological analysis also showed that the number and the caliber of lymphatic vessels were significantly greater at the DES edges compared with the control and DES+20 sites, whereas there was no significant difference between the control and the DES+20 sites. These results indicate that DES affect the number and the caliber of lymphatic vessels at the DES edges in the coronary adventitia in pigs.

Effects of Cardiac Lymphatic Vessel Ligation on Coronary Vasomotion in Pigs In Vivo

We have previously demonstrated that adventitial inflammation associated with Rho-kinase activation plays important roles in the pathogenesis of coronary artery spasm and DES-induced coronary hyperconstricting responses in pigs and humans.[1,8,12–14,25,26] DES implantation enhances chronic adventitial inflammation associated with enhanced VV formation, sympathetic nerve fiber formation, macrophage infiltration, and Rho-kinase activation.[1,7] Notably, the adventitia harbors 2 types of vessels, VV and lymphatic vessels.[15] In the protocol 1, enhanced formation of cardiac lymphatic vessels at the DES edges, but not at the BMS edges or nonstented sites, suggests that lymphatic vessels may be involved in the pathogenesis of coronary hyperconstricting responses after DES implantation. In the protocol 2, cardiac lymphatic vessels ligation enhanced coronary hyperconstricting responses associated with decreased coronary lymphatic vessels, hypertrophic adipocytes, enhanced inflammation in the adventitia, and Rho-kinase activation, whereas there was no significant difference in the number of VV or sympathetic nerve fibers between the 2 groups. Discrepancy between the coronary lymphatic vessels and VV formation in the protocol 2 may be because of their different healing processes in response to lymphatic vessels ligation injury and prolonged need of lymphatic vessels to drain excessive proteins and fluid compared with VV.[40]

In line with the present findings, lymphatic vessels were markedly decreased in lymphatic edematous tail of mice.[41] Adipocyte hypertrophy was initiated by lymphatic dysfunction,[42] and hypertrophic adipose tissue in obese mice mobilize inflammatory cells.[43] These structural and functional alterations of lymphatic vessels in responses to inflammation may also be the case for the heart in our body.[44] Indeed, inhibition of endogenous lymphangiogenesis increases cardiac inflammation in mice.[45] We previously demonstrated that reduced adiponectin level is associated with enhanced macrophage infiltration in visceral adipose tissue in mice.[46] We have recently demonstrated that reduced adiponectin and enlarged adipocyte size are associated with enhanced macrophage infiltration in the coronary adventitia and enhanced coronary hyperconstricting responses in pigs in vivo.[25]

In the present study, the number of lymphatic vessels and adipocyte size were associated with the extent of local inflammation (IL-1β-positive cells) and Rho-kinase activity. Indeed, we have previously demonstrated that IL-1β increases Rho-kinase activity in human coronary vascular smooth muscle cells in vitro[47] and that chronic treatment with IL-1β in the coronary adventitia induces coronary vasospasm through Rho-kinase activation in pigs in vivo.[12] Taken together, in the protocol 1, although compensated lymphangiogenesis occurred in the coronary adventitia, it is possible that the extent of compensatory lymphangiogenesis was not enough to suppress adventitial inflammation. In the protocol 2, it is conceivable that reduced cardiac lymphatic vessels with hypertrophic adipocytes lead to chronic adventitial inflammation and enhances Rho-kinase activity, resulting in coronary hyperconstricting responses. Coronary adventitia harbors several components, including VV, lymphatic vessels, macrophages, and adipocytes. When lymphatic dysfunction occurs, lymph stasis and decreased number of lymphatic vessels are noted, associated with adipocyte hypertrophy and infiltration of inflammatory cells, such as macrophages and IL-1β–positive cells, in the coronary adventitia. IL-1β can enhance Rho-kinase activity in the medial vascular smooth muscle cells, resulting in enhanced coronary hyperconstricting responses. Taken together, cardiac lymphatic vessel dysfunction plays important roles in the pathogenesis of coronary spasm and cardiac structural changes (see Graphic Abstract).

We found that the lymphatic flow of ICG was obstructed even at 6 weeks after the lymphatic vessels ligation. This finding suggests that lymphatic flow remained impaired in the ligation group for at least 6 weeks after the operation. Indeed, in the present study, we also confirmed that myocardial fibrosis and thickening of tricuspid and mitral valves were evident in the ligation group compared with the sham group. Consistent with the present findings, it was previously reported that fibrosis was commonly noted in lymphedematous tissue[48–51] and in the rabbit heart with cardiac lymph obstruction[52] and that cardiac lymphatic obstruction also induced thickening of atrioventricular valves in dogs.[53] Our findings are consistent with the previous findings, suggesting that our ligation technique was enough to obstruct lymphatic flow.

Clinical Implications

Lymphatic vessels may play important roles in the pathogenesis of many disorders, including lymphedema, inflammation, transplant rejection, cancer, and cardiovascular disease.[44,54] Accelerated cardiac lymphangiogenesis with VEGF-C improved myocardial fluid balance, cardiac inflammation, fibrosis, and functions.[55,56] Moreover, increased lymphatic vessels were noted with cardiac pathological changes, including myocarditis and myocardial hypertrophy in the human autopsy hearts.[37] However, the roles of cardiac lymphatic vessels in the pathogenesis of coronary vasomotion abnormalities remain to be elucidated. In the present study, we were able to provide evidence that functional and structural alterations of cardiac lymphatic vessels are substantially involved in the pathogenesis of coronary vasomotion abnormalities in pigs in vivo. Recent large-scale trial demonstrated that ≈30% of patients have unremitting angina until 1 year after successful percutaneous coronary intervention with DES.[5] Notably, some patients suffer from enhanced coronary hyperconstricting responses after DES implantation.[2,6] In addition, a lack of hemodynamically significant coronary artery obstruction is noted in about 20% to 40% of patients with

angina and a positive stress test.[57] Intractable vasospastic angina is also an emerging therapeutic target.[58] Based on the present findings, coronary lymphatic vessels could be regarded as a new therapeutic target for coronary vasomotion disorders.

Study Limitations

Several study limitations should be mentioned for the present study. First, it was previously reported that not only cardiac lymphatic vessels but also pretracheal lymph nodes could be ligated in dogs.[28] In the present study, for technical reasons, it was difficult to ligate pretracheal lymph nodes in pigs in vivo. However, our technique of cardiac lymphatic vessels ligation was enough to create lymph flow obstruction as confirmed in the ICG study at 6 weeks after the procedure. Second, because we were unable to clearly see the lymphatic vessels because of their small size without blood color, it was difficult to determine the orientation of lymphatic vessels when making paraffin sections. Third, it was also difficult to perform immunostainings of resin-embedded sections of the stent implantation site, which makes it hard to reveal the whole topology of lymphatic vessels of the stented arterial segment. However, it is important to address the morphometry of lymphatic vessels at the stented coronary arteries for further mechanistic insights in future studies. Fourth, ligation of lymphatic vessels could injure the adventitial sympathetic nerve fibers because we were unable to clearly recognize adventitial nerves in vivo during the ligation procedure. We have recently demonstrated that there are significant correlations between sympathetic nerve fibers and coronary hyperconstricting responses.[26] However, in the present study, quantitative histological analysis showed that there was no significant difference in the number of adventitial sympathetic nerve fibers between the sham and the ligation groups in the protocol 2. Fifth, we used only male pigs in the present study to eliminate potential hormonal changes during menstruation period and to consider coronary risks.[59–61] However, we previously demonstrated that this male pig model has coronary vasomotion abnormalities.[3,7,12,25–27,62–65]

Conclusions

The present study provides evidence that cardiac lymphatic vessels dysfunction plays important roles in the pathogenesis of coronary hyperconstricting responses.

Acknowledgments

We thank Y. Watanabe for her excellent technical assistance and Asahi Kasei Pharma for providing hydroxyfasudil.

Sources of Funding

This work was supported, in part, by the grants-in-aid for the Scientific Research (18890018) and the Global COE Project (F02) and the grants-in-aid (H22-Shinkin-004) from the Japanese Ministry of Education, Culture, Sports, Science, and Technology, Tokyo, Japan.

Disclosures

None.

References

1. Shimokawa H. 2014 Williams Harvey Lecture: importance of coronary vasomotion abnormalities-from bench to bedside. *Eur Heart J*. 2014;35:3180–3193. doi: 10.1093/eurheartj/ehu427
2. Aizawa K, Yasuda S, Takahashi J, Takii T, Kikuchi Y, Tsuburaya R, Ito Y, Ito K, Nakayama M, Takeda M, Shimokawa H. Involvement of rho-kinase activation in the pathogenesis of coronary hyperconstricting responses induced by drug-eluting stents in patients with coronary artery disease. *Circ J*. 2012;76:2552–2560.
3. Tsuburaya R, Yasuda S, Shiroto T, Ito Y, Gao JY, Aizawa K, Kikuchi Y, Ito K, Takahashi J, Ishibashi-Ueda H, Shimokawa H. Long-term treatment with nifedipine suppresses coronary hyperconstricting responses and inflammatory changes induced by paclitaxel-eluting stent in pigs in vivo: possible involvement of Rho-kinase pathway. *Eur Heart J*. 2012;33:791–799. doi: 10.1093/eurheartj/ehr145
4. Ong P, Athanasiadis A, Perne A, Mahrholdt H, Schäufele T, Hill S, Sechtem U. Coronary vasomotor abnormalities in patients with stable angina after successful stent implantation but without in-stent restenosis. *Clin Res Cardiol*. 2014;103:11–19. doi: 10.1007/s00392-013-0615-9
5. Serruys PW, Chevalier B, Dudek D, et al. A bioresorbable everolimus-eluting scaffold versus a metallic everolimus-eluting stent for ischaemic heart disease caused by de-novo native coronary artery lesions (ABSORB II): an interim 1-year analysis of clinical and procedural secondary outcomes from a randomised controlled trial. *Lancet*. 2015;385:43–54. doi: 10.1016/S0140-6736(14)61455-0
6. Brott BC, Anayiotos AS, Chapman GD, Anderson PG, Hillegass WB. Severe, diffuse coronary artery spasm after drug-eluting stent placement. *J Invasive Cardiol*. 2006;18:584–592.
7. Shiroto T, Yasuda S, Tsuburaya R, Ito Y, Takahashi J, Ito K, Ishibashi-Ueda H, Shimokawa H. Role of Rho-kinase in the pathogenesis of coronary hyperconstricting responses induced by drug-eluting stents in pigs in vivo. *J Am Coll Cardiol*. 2009;54:2321–2329. doi: 10.1016/j.jacc.2009.07.045
8. Nishimiya K, Matsumoto Y, Shindo T, Hanawa K, Hasebe Y, Tsuburaya R, Shiroto T, Takahashi J, Ito K, Ishibashi-Ueda H, Yasuda S, Shimokawa H. Association of adventitial vasa vasorum and inflammation with coronary hyperconstriction after drug-eluting stent implantation in pigs in vivo. *Circ J*. 2015;79:1787–1798. doi: 10.1253/circj.CJ-15-0149
9. Kandabashi T, Shimokawa H, Miyata K, Kunihiro I, Kawano Y, Fukata Y, Higo T, Egashira K, Takahashi S, Kaibuchi K, Takeshita A. Inhibition of myosin phosphatase by upregulated rho-kinase plays a key role for coronary artery spasm in a porcine model with interleukin-1beta. *Circulation*. 2000;101:1319–1323.
10. Shimokawa H, Takeshita A. Rho-kinase is an important therapeutic target in cardiovascular medicine. *Arterioscler Thromb Vasc Biol*. 2005;25:1767–1775. doi: 10.1161/01.ATV.0000176193.83629.c8
11. Lanza GA, Careri G, Crea F. Mechanisms of coronary artery spasm. *Circulation*. 2011;124:1774–1782. doi: 10.1161/CIRCULATIONAHA.111.037283
12. Shimokawa H, Ito A, Fukumoto Y, Kadokami T, Nakaike R, Sakata M, Takayanagi T, Egashira K, Takeshita A. Chronic treatment with interleukin-1 beta induces coronary intimal lesions and vasospastic responses in pigs in vivo. The role of platelet-derived growth factor. *J Clin Invest*. 1996;97:769–776. doi: 10.1172/JCI118476
13. Ohyama K, Matsumoto Y, Takanami K, et al. Coronary adventitial and perivascular adipose tissue inflammation in patients with vasospastic angina. *J Am Coll Cardiol*. 2018;71:414–425. doi: 10.1016/j.jacc.2017.11.046
14. Nishimiya K, Matsumoto Y, Takahashi J, Uzuka H, Wang H, Tsuburaya R, Hao K, Ohyama K, Odaka Y, Miyata S, Ito K, Shimokawa H. Enhanced adventitial vasa vasorum formation in patients with vasospastic angina: assessment with OFDI. *J Am Coll Cardiol*. 2016;67:598–600. doi: 10.1016/j.jacc.2015.11.031
15. Aspelund A, Robciuc MR, Karaman S, Makinen T, Alitalo K. Lymphatic system in cardiovascular medicine. *Circ Res*. 2016;118:515–530. doi: 10.1161/CIRCRESAHA.115.306544
16. Margaris KN, Black RA. Modelling the lymphatic system: challenges and opportunities. *J R Soc Interface*. 2012;9:601–612. doi: 10.1098/rsif.2011.0751
17. Baluk P, Tammela T, Ator E, Lyubynska N, Achen MG, Hicklin DJ, Jeltsch M, Petrova TV, Pytowski B, Stacker SA, Ylä-Herttuala S, Jackson DG, Alitalo K, McDonald DM. Pathogenesis of persistent lymphatic vessel hyperplasia in chronic airway inflammation. *J Clin Invest*. 2005;115:247–257. doi: 10.1172/JCI22037
18. Huggenberger R, Ullmann S, Proulx ST, Pytowski B, Alitalo K, Detmar M. Stimulation of lymphangiogenesis via VEGFR-3 inhibits chronic skin inflammation. *J Exp Med*. 2010;207:2255–2269. doi: 10.1084/jem.20100559
19. Vuorio T, Tirronen A, Ylä-Herttuala S. Cardiac lymphatics—a new avenue for therapeutics? *Trends Endocrinol Metab*. 2017;28:285–296. doi: 10.1016/j.tem.2016.12.002

20. Cui Y. The role of lymphatic vessels in the heart. *Pathophysiology*. 2010;17:307–314. doi: 10.1016/j.pathophys.2009.07.006
21. Drozdz K, Janczak D, Dziegiel P, Podhorska M, Piotrowska A, Patrzalek D, Andrzejak R, Szuba A. Adventitial lymphatics and atherosclerosis. *Lymphology*. 2012;45:26–33.
22. Kutkut I, Meens MJ, McKee TA, Bochaton-Piallat ML, Kwak BR. Lymphatic vessels: an emerging actor in atherosclerotic plaque development. *Eur J Clin Invest*. 2015;45:100–108. doi: 10.1111/eci.12372
23. Bradham RR, Parker EF. The cardiac lymphatics. *Ann Thorac Surg*. 1973;15:526–535.
24. Eriksson G. [Olaus Rudbeck as scientist and professor of medicine]. *Sven Med Tidskr*. 2004;8:39–44.
25. Ohyama K, Matsumoto Y, Amamizu H, Uzuka H, Nishimiya K, Morosawa S, Hirano M, Watabe H, Funaki Y, Miyata S, Takahashi J, Ito K, Shimokawa H. Association of coronary perivascular adipose tissue inflammation and drug-eluting stent-induced coronary hyperconstricting responses in pigs: 18F-fluorodeoxyglucose positron emission tomography imaging study. *Arterioscler Thromb Vasc Biol*. 2017;37:1757–1764. doi: 10.1161/ATVBAHA.117.309843
26. Uzuka H, Matsumoto Y, Nishimiya K, et al. Renal denervation suppresses coronary hyperconstricting responses after drug-eluting stent implantation in pigs in vivo through the kidney-brain-heart axis. *Arterioscler Thromb Vasc Biol*. 2017;37:1869–1880. doi: 10.1161/ATVBAHA.117.309777
27. Nishimiya K, Matsumoto Y, Uzuka H, Ogata T, Hirano M, Shindo T, Hasebe Y, Tsuburaya R, Shiroto T, Takahashi J, Ito K, Shimokawa H. Beneficial effects of a novel bioabsorbable polymer coating on enhanced coronary vasoconstricting responses after drug-eluting stent implantation in pigs in vivo. *JACC Cardiovasc Interv*. 2016;9:281–291. doi: 10.1016/j.jcin.2015.09.041
28. Ludwig LL, Schertel ER, Pratt JW, McClure DE, Ying AJ, Heck CF, Myerowitz PD. Impairment of left ventricular function by acute cardiac lymphatic obstruction. *Cardiovasc Res*. 1997;33:164–171.
29. van der Wal A, de Mol B. Feasibility of mapping and cannulation of the porcine epicardial lymphatic system for sampling and decompression in heart failure research. *J Clin Transl Res*. 2018;4:2.
30. Mihara M, Hara H, Araki J, Kikuchi K, Narushima M, Yamamoto T, Iida T, Yoshimatsu H, Murai N, Mitsui K, Okitsu T, Koshima I. Indocyanine green (ICG) lymphography is superior to lymphoscintigraphy for diagnostic imaging of early lymphedema of the upper limbs. *PLoS One*. 2012;7:e38182. doi: 10.1371/journal.pone.0038182
31. Bouta EM, Wood RW, Brown EB, Rahimi H, Ritchlin CT, Schwarz EM. *In vivo* quantification of lymph viscosity and pressure in lymphatic vessels and draining lymph nodes of arthritic joints in mice. *J Physiol*. 2014;592:1213–1223. doi: 10.1113/jphysiol.2013.266700
32. Osman OS, Selway JL, Kępczyńska MA, Stocker CJ, O'Dowd JF, Cawthorne MA, Arch JR, Jassim S, Langlands K. A novel automated image analysis method for accurate adipocyte quantification. *Adipocyte*. 2013;2:160–164. doi: 10.4161/adip.24652
33. Noblet JN, Owen MK, Goodwill AG, Sassoon DJ, Tune JD. Lean and obese coronary perivascular adipose tissue impairs vasodilation via differential inhibition of vascular smooth muscle K+ channels. *Arterioscler Thromb Vasc Biol*. 2015;35:1393–1400. doi: 10.1161/ATVBAHA.115.305500
34. Koczor CA, Torres RA, Fields E, Qin Q, Park J, Ludaway T, Russ R, Lewis W. Transgenic mouse model with deficient mitochondrial polymerase exhibits reduced state IV respiration and enhanced cardiac fibrosis. *Lab Invest*. 2013;93:151–158. doi: 10.1038/labinvest.2012.146
35. Matsumoto Y, Adams V, Jacob S, Mangner N, Schuler G, Linke A. Regular exercise training prevents aortic valve disease in low-density lipoprotein-receptor-deficient mice. *Circulation*. 2010;121:759–767. doi: 10.1161/CIRCULATIONAHA.109.892224
36. Banziger-Tobler NE, Halin C, Kajiya K, Detmar M. Growth hormone promotes lymphangiogenesis. *Am J Pathol*. 2008;173:586–597. doi: 10.2353/ajpath.2008.080060
37. Kholová I, Dragneva G, Cermáková P, Laidinen S, Kaskenpää N, Hazes T, Cermáková E, Steiner I, Ylä-Herttuala S. Lymphatic vasculature is increased in heart valves, ischaemic and inflamed hearts and in cholesterol-rich and calcified atherosclerotic lesions. *Eur J Clin Invest*. 2011;41:487–497. doi: 10.1111/j.1365-2362.2010.02431.x
38. Nishimiya K, Matsumoto Y, Uzuka H, et al. Accuracy of optical frequency domain imaging for evaluation of coronary adventitial vasa vasorum formation after stent implantation in pigs and humans—a validation study. *Circ J*. 2015;79:1323–1331. doi: 10.1253/circj.CJ-15-0078
39. Muley A, Odaka Y, Lewkowich IP, Vemaraju S, Yamaguchi TP, Shawber C, Dickie BH, Lang RA. Myeloid Wnt ligands are required for normal development of dermal lymphatic vasculature. *PLoS One*. 2017;12:e0181549. doi: 10.1371/journal.pone.0181549
40. Ishikawa Y, Akishima-Fukasawa Y, Ito K, Akasaka Y, Tanaka M, Shimokawa R, Kimura-Matsumoto M, Morita H, Sato S, Kamata I, Ishii T. Lymphangiogenesis in myocardial remodelling after infarction. *Histopathology*. 2007;51:345–353. doi: 10.1111/j.1365-2559.2007.02785.x
41. Shimizu Y, Shibata R, Ishii M, Ohashi K, Kambara T, Uemura Y, Yuasa D, Kataoka Y, Kihara S, Murohara T, Ouchi N. Adiponectin-mediated modulation of lymphatic vessel formation and lymphedema. *J Am Heart Assoc*. 2013;2:e000438. doi: 10.1161/JAHA.113.000438
42. Harvey NL. The link between lymphatic function and adipose biology. *Ann N Y Acad Sci*. 2008;1131:82–88. doi: 10.1196/annals.1413.007
43. Mori J, Patel VB, Abo Alrob O, Basu R, Altamimi T, Desaulniers J, Wagg CS, Kassiri Z, Lopaschuk GD, Oudit GY. Angiotensin 1-7 ameliorates diabetic cardiomyopathy and diastolic dysfunction in db/db mice by reducing lipotoxicity and inflammation. *Circ Heart Fail*. 2014;7:327–339. doi: 10.1161/CIRCHEARTFAILURE.113.000672
44. Huang LH, Lavine KJ, Randolph GJ. Cardiac lymphatic vessels, transport, and healing of the infarcted heart. *JACC Basic Transl Sci*. 2017;2:477–483. doi: 10.1016/j.jacbts.2017.02.005
45. Shimizu Y, Polavarapu R, Eskla KL, Pantner Y, Nicholson CK, Ishii M, Brunnhoelzl D, Mauria R, Husain A, Naqvi N, Murohara T, Calvert JW. Impact of lymphangiogenesis on cardiac remodeling after ischemia and reperfusion injury. *J Am Heart Assoc*. 2018;7:e009565. doi: 10.1161/JAHA.118.009565
46. Nakajima S, Ohashi J, Sawada A, Noda K, Fukumoto Y, Shimokawa H. Essential role of bone marrow for microvascular endothelial and metabolic functions in mice. *Circ Res*. 2012;111:87–96. doi: 10.1161/CIRCRESAHA.112.270215
47. Hiroki J, Shimokawa H, Higashi M, Morikawa K, Kandabashi T, Kawamura N, Kubota T, Ichiki T, Amano M, Kaibuchi K, Takeshita A. Inflammatory stimuli upregulate Rho-kinase in human coronary vascular smooth muscle cells. *J Mol Cell Cardiol*. 2004;37:537–546. doi: 10.1016/j.yjmcc.2004.05.008
48. Lynch LL, Mendez U, Waller AB, Gillette AA, Guillory RJ II, Goldman J. Fibrosis worsens chronic lymphedema in rodent tissues. *Am J Physiol Heart Circ Physiol*. 2015;308:H1229–H1236. doi: 10.1152/ajpheart.00527.2013
49. Li K, Zhang Z, Liu NF, Sadigh P, Evans VJ, Zhou H, Gao W, Zhang YX. Far-infrared radiation thermotherapy improves tissue fibrosis in chronic extremity lymphedema. *Lymphat Res Biol*. 2018;16:248–257. doi: 10.1089/lrb.2016.0057
50. Sun D, Yu Z, Chen J, Wang L, Han L, Liu N. The value of using a SkinFibroMeter for diagnosis and assessment of secondary lymphedema and associated fibrosis of lower limb skin. *Lymphat Res Biol*. 2017;15:70–76. doi: 10.1089/lrb.2016.0029
51. Ridner SH, Dietrich MS, Niermann K, Cmelak A, Mannion K, Murphy B. A prospective study of the lymphedema and fibrosis continuum in patients with head and neck cancer. *Lymphat Res Biol*. 2016;14:198–205. doi: 10.1089/lrb.2016.0001
52. Kong D, Kong X, Wang L. Effect of cardiac lymph flow obstruction on cardiac collagen synthesis and interstitial fibrosis. *Physiol Res*. 2006;55:253–258.
53. Okada E, Shozawa T. Mucoid degeneration of the atrioventricular valve caused by cardiac lymphostasis: an experimental study in dogs. *Cardiovasc Pathol*. 1994;3:163–166. doi: 10.1016/1054-8807(94)90025-6
54. Padera TP, Meijer EF, Munn LL. The lymphatic system in disease processes and cancer progression. *Annu Rev Biomed Eng*. 2016;18:125–158. doi: 10.1146/annurev-bioeng-112315-031200
55. Henri O, Pouehe C, Houssari M, Galas L, Nicol L, Edwards-Lévy F, Henry JP, Dumesnil A, Boukhalfa I, Banquet S, Schapman D, Thuillez C, Richard V, Mulder P, Brakenhielm E. Selective stimulation of cardiac lymphangiogenesis reduces myocardial edema and fibrosis leading to improved cardiac function following myocardial infarction. *Circulation*. 2016;133:1484–1497; discussion 1497. doi: 10.1161/CIRCULATIONAHA.115.020143
56. Vieira JM, Norman S, Villa Del Campo C, Cahill TJ, Barnette DN, Gunadasa-Rohling M, Johnson LA, Greaves DR, Carr CA, Jackson DG, Riley PR. The cardiac lymphatic system stimulates resolution of inflammation following myocardial infarction. *J Clin Invest*. 2018;128:3402–3412. doi: 10.1172/JCI97192
57. Crea F, Bairey Merz CN, Beltrame JF, Berry C, Camici PG, Kaski JC, Ong P, Pepine CJ, Sechtem U, Shimokawa H. Mechanisms and diagnostic evaluation of persistent or recurrent angina following percutaneous coronary revascularization [published online January 4, 2019]. *Eur Heart J*. doi:10.1093/Eurheartj/ehy857

58. Beltrame JF, Crea F, Kaski JC, Ogawa H, Ong P, Sechtem U, Shimokawa H, Bairey Merz CN; Coronary Vasomotion Disorders International Study Group (COVADIS). The who, what, why, when, how and where of vasospastic angina. *Circ J*. 2016;80:289–298. doi: 10.1253/circj.CJ-15-1202
59. Adachi Y, Ikeda N, Sakakura K, Netsu S, Ibe T, Wada H, Momomura S, Fujita H. Intractable coronary spastic angina improvement after continuous combined estrogen-progestin hormonal contraception use in a premenopausal woman. *Intern Med*. 2016;55:2639–2642. doi: 10.2169/internalmedicine.55.6947
60. Hiroki J, Shimokawa H, Mukai Y, Ichiki T, Takeshita A. Divergent effects of estrogen and nicotine on Rho-kinase expression in human coronary vascular smooth muscle cells. *Biochem Biophys Res Commun*. 2005;326:154–159. doi: 10.1016/j.bbrc.2004.11.011
61. Kawana A, Takahashi J, Takagi Y, et al; Japanese Coronary Spasm Association. Gender differences in the clinical characteristics and outcomes of patients with vasospastic angina–a report from the Japanese Coronary Spasm Association. *Circ J*. 2013;77:1267–1274.
62. Shimokawa H, Tomoike H, Nabeyama S, Yamamoto H, Araki H, Nakamura M, Ishii Y, Tanaka K. Coronary artery spasm induced in atherosclerotic miniature swine. *Science*. 1983;221:560–562.
63. Shimokawa H, Vanhoutte PM. Angiographic demonstration of hyperconstriction induced by serotonin and aggregating platelets in porcine coronary arteries with regenerated endothelium. *J Am Coll Cardiol*. 1991;17:1197–1202.
64. Ito A, Egashira K, Kadokami T, Fukumoto Y, Takayanagi T, Nakaike R, Kuga T, Sueishi K, Shimokawa H, Takeshita A. Chronic inhibition of endothelium-derived nitric oxide synthesis causes coronary microvascular structural changes and hyperreactivity to serotonin in pigs. *Circulation*. 1995;92:2636–2644.
65. Shimokawa H, Morishige K, Miyata K, Kandabashi T, Eto Y, Ikegaki I, Asano T, Kaibuchi K, Takeshita A. Long-term inhibition of Rho-kinase induces a regression of arteriosclerotic coronary lesions in a porcine model in vivo. *Cardiovasc Res*. 2001;51:169–177.

Highlights

- The major findings of the present study were as follows: (1) Enhanced lymphatic vessel formation was noted at the drug-eluting stent edges associated with coronary vasoconstricting responses but not at the bare metal stent edges or sites apart from drug-eluting stent. (2) Lymphatic vessels ligation further enhanced coronary hyperconstricting responses after drug-eluting stent implantation. (3) Lymphatic vessels ligation decreased the number of lymphatic vessels, although there were no significant differences in the number of vasa vasorum between the sham and the ligation groups. (4) Lymphatic vessels ligation caused adipocyte hypertrophy associated with enhanced inflammation in the adventitia and Rho-kinase activation. The present study provides evidence that cardiac lymphatic vessels dysfunction plays important roles in the pathogenesis of coronary spasm and cardiac structural changes.